Journal Name

ARTICLE

Compatibility Balanced Antibacterial Modification Based on Vapor-Deposited Parylene Coatings for Biomaterials

Chih-Hao Chang,[a] Shu-Yun Yeh,[b,±] Bing-Heng Lee,[a,±] Che-Wei Hsu,[a] Yung-Chih Chen,[b] Chia-Jie Chen,[a] Ting-Ju Lin,[b] Mark Hung-Chih Chen,[a] Ching-Tsan Huang,[c] Hsien-Yeh Chen[b,*]

Advanced antibacterial surfaces are designed based on covalently attached antibacterial agents, avoiding potential side effects associated with overdosed or eluted agents. The technique is widely applicable regardless of the underlying substrate material. In addition, antibacterial surfaces are effective against the early stage of bacterial adhesion and can significantly reduce the formation of biofilm, without compromising biocompatibility. Here, this concept was realized by employing a benzoyl-functionalized parylene coating. The antibacterial agent chlorhexidine was used as a proof of concept. Chlorhexidine was immobilized by reaction with photoactivated benzoyl-functionalized surfaces, including titanium alloy, stainless steel, polyether ether ketone, polymethyl methacrylate, and polystyrene. A low concentration of chlorhexidine (1.4 ± 0.08 nmol·cm^{-2}) covalently bound to surfaces rendered them sufficiently resistant to an *Enterobacter cloacae* inoculum and its adherent biofilm. Compared to unmodified surfaces, up to a 30-fold reduction in bacterial attachment was achieved with this coating technology. The immobilization of chlorhexidine was verified with infrared reflection absorption spectroscopy (IRRAS) and X-ray photoelectron spectroscopy (XPS), and a leaching test was performed to confirm that the chlorhexidine molecules were not dislodged. Cell compatibility was examined by culturing fibroblasts and osteoblasts on the modified surfaces, revealing greater than 93% cell viability. This coating technology may be broadly applicable for a wide range of other antibacterial agents and allow the design of new biomaterials.

Introduction

Infections by microorganisms present on invasive medical devices create a broad spectrum of nosocomial pathologies [1] and are a primary cause of severe inflammation, which can damage surrounding tissue, result in device failure, and potentially lead to patient morbidity and death [2]. These infections commonly result from the irreversible adhesion of bacteria to a device surface, which then enters the wound site and leads to the formation of complex communities of a biofilms [3, 4]. Surface modification is a relatively straightforward strategy to prevent device-associated infection (DAI) [5, 6]. This strategy involves the modification of the interfacial properties of a medical device without disrupting its underlying bulk properties. Modification of the device surface can prevent DAI at the implantation site, where access by intravenously administered antibiotics is impeded [7]. Surface modifications are commonly performed in three ways. In the first approach, the

modifications are designed to reduce bacterial attachment or viability. For example, polyethylene glycol (PEG) and its derivatives can be used to prevent the adsorption of non-specifically accumulated serum proteins that promote bacterial adherence and colonization [8], or active biomolecules such as the cell-adhering peptide Arg-Gly-Asp (RGD) can be coupled to the surface to promote the adhesion of host cells to the device surface, thus preventing bacterial growth [7, 9]. However, these methods do not prevent the adhesion of bacteria and biofilms after longer periods of time [10, 11]. In the second approach, surfaces are designed to eradicate bacteria before colonization by releasing antibacterial species or antiseptic materials, such as chlorhexidine [12], triclosan [13], metal ions [14], or combinations of these materials [15]. There are, however, numerous problems regarding the leaching of antibiotic agents; the uses of these antibiotic/antiseptic materials are limited by their toxicity [16] and allergenicity [17]. In addition, the elution of

antibiotic/antiseptic materials will eventually taper to ineffective concentrations [18], and the eluting low-concentration antibiotics could result in the emergence of resistant organisms [19]. The final approach involves the covalent attachment of cationic antimicrobials that are able to disrupt the bacterial cell membrane [20]. However, grafting techniques are conducted on a case-by-case basis using selected substrate materials and usually require an extensive knowledge of surface chemistry. Novel antibacterial treatments for biomedical devices should do the following: (i) avoid the leaching of materials to surrounding biological environments, thus alleviating any concerns about damaging cells and tissues; (ii) be applicable to a wide range of substrate materials without needing substantial material science or surface chemistry knowledge to apply these modifications; and (iii) enable the covalent attachment of antibacterial materials for long-term performance to reduce bacterial attachment.

In this report, we sought to realize this concept by using a facile and effective antimicrobial coating technology based on a photodefinable parylene coating, poly(4-benzoyl-*p*-xylylene-*co-p*-xylylene), hereafter referred to as benzoyl-PPX, to covalently immobilize antibacterial materials. Chlorhexidine (CHX) is a commonly used antibacterial agent [21] that damages bacterial cells by destabilizing the cell wall and the cytoplasmic membrane, eventually eliciting cell death [22, 23]. As a proof of concept, CHX was immobilized on the benzoyl-PPX coating applied to various substrates, including titanium alloy (Ti6Al4V), stainless steel (SS), polyether ether ketone (PEEK), polymethyl methacrylate (PMMA), and polystyrene (PS). Benzoyl-PPX can be prepared through chemical vapor deposition (CVD) polymerization on a wide range of different substrates/materials that are used in microcolloids [24], stents [25], and microfluidic devices [26]. The coating's photoactivated carbonyl groups can facilitate light-induced molecular crosslinking via insertion into C-H or N-H bonds upon photo-illumination at 365 nm [26, 27]. An *Enterobacter cloacae* (*E. cloacae*) biofilm was used as a model in this study to evaluate antimicrobial activity on these modified surfaces. Important issues, including the potential detachment of coated materials from the modified surface and the viability of normal cells exposed to these antimicrobial surfaces, are also discussed in this report.

Experimental

Materials

The following materials were obtained commercially and used as received unless otherwise noted: [2,2]paracyclophane (Jiangsu Miaoqiao Synthesis Chemical, China, 98%), aluminum chloride (Alfa Aesar, 99%), benzoyl chloride (Alfa Aesar, 99%), dichloromethane (Macron Chemicals, USA), anhydrous magnesium sulfate (J.T. Baker, USA, 99.5%), chlorhexidine dihydrochloride (Sigma Aldrich, 98%), titanium alloy (Ti6Al4V, Titanium Industries, USA), polymethyl

methacrylate (PMMA, Taifonacrylic, Taiwan), polyether ether ketone (PEEK, Link Upon Advanced Material Corp., Taiwan), polystyrene (PS, Taifonacrylic, Taiwan), stainless steel (SS, Structure Probe, USA), and silicon wafers (Goldeninent, Taiwan). Gold substrates were fabricated on a 4-inch silicon wafer by depositing a 300-Å layer of titanium followed by a 700-Å layer of gold with a thermal evaporator (Kao Duen Technology, Taiwan). In order to avoid contaminations, all silicon substrates were cleaned using a piranha solution (3:1 v/v $H_2SO_4:H_2O_2$) right before use.

CVD polymerization and photoimmobilization

The starting material, 4-benzoyl[2,2]paracyclophane, was synthesized according to previously reported methods [28]. Approximately 500 mg of the material was used for CVD polymerization in a self-designed CVD system that comprises a sublimation zone, a pyrolysis zone, and a deposition chamber. 4-Benzoyl[2,2]paracyclophane was first sublimated in the sublimation zone at approximately 125 °C. The sublimated species was then transferred in a stream of argon carrier gas at a flow rate of 30 sccm to the pyrolysis zone, in which the temperature was adjusted to 810 °C. Following pyrolysis, the radicals were transferred into the deposition chamber and then polymerized onto a rotating holder at 20 °C to ensure a uniform deposition of benzoyl-PPX; the chamber wall was held at 100 °C to prevent any residual deposition. A pressure of 75 mTorr was maintained throughout the CVD polymerization process, and all deposition rates were regulated at approximately 0.5 Å s^{-1}. Selected substrate materials including Ti6Al4V, SS, PEEK, PMMA, and PS were first cleaned using ethanol and were then used as substrates for CVD coating. The photoimmobilization process was performed by exposing samples to UV light (Univex, Taiwan) at a wavelength of approximately 365 nm and a maximum intensity of 65 mW·cm^{-2} for 5 min. Finally, the samples were rinsed thoroughly with deionized water and then gently dried with a stream of compressed nitrogen gas. Right after immobilization process, resulting samples were subjected to according antibacterial tests or cell viability tests.

Surface characterizations

Infrared reflection absorption spectroscopy (IRRAS) spectra were recorded using a Spectrum 100 FT-IR spectrometer (PerkinElmer, USA) equipped with an advanced grazing angle specular reflectance accessory (AGA, PIKE Technologies, USA) and a liquid nitrogen cooled MCT detector. The samples were mounted in a nitrogen-purged chamber, and the recorded spectra were corrected for any residual baseline drift. A theta probe X-ray photoelectron spectrometer (Thermal Scientific, UK) was employed for the X-ray photoelectron spectroscopy (XPS) using a monochromatized AlKα X-ray source. An X-ray power of 150 kW was used for all data acquisition, and the pass energies were adjusted to 200.0 eV, 20.0 eV and 20.0 eV for the survey scan, the high-resolution C_{1s} and the Cl_{2p} elemental scans, respectively. The atomic analysis of the XPS spectra was based on the atomic concentrations and was compared to the theoretical values calculated on the basis of the structure. A

quartz crystal microbalancing (QCM) analysis was performed using an affinity detection system (ADS) QCM instrument (ANT Technologies, Taiwan). The sensing element of the QCM instrument is a piezoelectric quartz disc with a resonant frequency of 9 MHz. For the experiment, resonant frequency changes were monitored at each of the following modification steps: bare crystal, after coating with benzoyl-PPX, and after the immobilization of CHX on benzoyl-PPX. The resulting concentration data were calculated based on a total sensing area of 0.1 cm^2. Coating adhesion strength was evaluated following a standard cross-cut tape test of ASTM D3359[29] that was performed using a multi-blade tester. Two perpendicular sets of scratches were created on the coated substrate, and Scotch tape was then applied and removed from the coatings within 0.5 to 1.0 seconds. The pulling angle was 60 degrees. ASTM D3359 classification of adhesion strength. (5B): the edges of the cuts are completely smooth, and none of the square or lattice is detached; (4B): less than 5% of the lattice is detached; (3B): 5 to 15% of the lattice is detached; (2B): 15 to 35% of the lattice is detached; (1B): 35 to 65% of the lattice is detached; (0B): flaking and detachment in excess of 65%.

Antimicrobial test

The pathogenic bacterial strain *E. cloacae* (ATCC 13047) was obtained from the Department of Clinical Laboratory, Sciences and Medical Biotechnology, College of Medicine, National Taiwan University, Taiwan and cultured in 1% tryptic soy broth (TSB, BD, USA) at 35°C. Measurements of bacterial growth were obtained following the protocol of the ISO 22196 standard test methods. *E. cloacae* bacteria were cultured overnight in 1% tryptic soy broth (TSB, BD, USA) and were diluted to 1×10^7 CFU mL^{-1} in growth medium. 200 μL of the diluted bacteria solutions were then applied to CHX-benzoyl-PPX-modified substrates including Ti6Al4V, SS, PEEK, PMMA, and PS; unmodified such substrates were also used parallelly during the test, as control samples. 1 cm^2 square-shaped sample was used as a standard for all samples tested in the experiments. A separate experiment was conducted to culture *E. cloacae* bacteria in media containing 10% fetal bovine serum (FBS) for 24 hrs at 37 °C in a humidified atmosphere of 5% CO$_2$ and 95% air, in order to verify the antibacterial activity in such a medium. Tested samples were incubated under static conditions at 35°C during 24-hr time frame. Finally, suspensions of bacteria were harvested from the sample surfaces and placed in unmodified cell culture plates (96-well, Corning, USA) for analysis. Bacterial density was monitored at 600 nm (OD$_{600}$) using a multi-well plate reader (PowerWave X, BioTek Instruments, USA). Each data point was obtained by averaging three replicates of test samples. After 24 hrs, the bacterial suspensions were collected from the surface of the test samples and then stained using the BacLight LIVE/DEAD bacterial viability kit (Life Technologies, USA). The resulting samples were visualized using an Axio Scope.A1 fluorescence microscope (Zeiss, Germany) with an Omega filter XF25 (Omega Optical, USA).

Biofilm formation

E. cloacae biofilms were developed in a modified drip-draw reactor[30] fabricated using a 500-ml polypropylene container (Nalgene, USA). The container, tubing, valves, and devices were washed, assembled and sterilized prior to each experiment. The assembly of the reactor was performed in a laminar air flow cabinet to prevent further contamination, and CHX-benzoyl-PPX-modified and unmodified substrates were placed in the reactor after the assembly. Biofilm formation was conducted following reported procedures[31, 32] and was implemented with an initial seeding density of 10^7 cells/ml *E. cloacae* in 1% TSB for at ambient temperature for 24 hrs. Subsequently, sterilized TSB at room temperature was constantly supplied to the reactor system at a constant flow rate of 540-600 ml/h for another 24 hrs. A peristaltic pump (Masterflex L/S Easy-Load II, Cole-Parmer, USA) was used to control the in-and-out flow rate of the reactor. The resulting samples were retrieved from the reactor and washed with PBS buffer solution. The formed biofilm on the surfaces of tested samples was harvested by vagarious vortex. Verification of the resulting biofilm was performed separately by using a crystal violet assay following previous reports[33, 34], and was recorded during a 48-hr time frame (12 hrs, 24 hrs, and 48 hrs). After forming a biofilm on the tested substrates of CHX-benzoyl-PPX-modified PMMA and Ti6Al4V (unmodified PMMA and Ti6Al4V were used as control surfaces), a fixation procedure of the resulting biofilm was performed by incubating the samples with 150 μL methanol for 15 min followed by incubation of crystal violet solution (0.1%, 150 μL, Sigma Aldrich, USA) for 20 min. Finally, a release process of the crystal violet assay was conducted by incubating the resulting samples with acetic acid (33%, 150 μL, Sigma Aldrich, USA) for 20 min, and the absorbance was measured at 590 nm by using a BioTek PowerWave reader (BioTek Instruments, USA). The colony formation unit per unit area (CFU·cm^{-2}) of the resulting biofilm was calculated using viable plate counting[35, 36] and was plotted based on logarithmic units (log$_{10}$·CFU·cm^{-2}). Experiments were performed in triplicate. Samples for scanning electron microscopy (SEM) imaging were retrieved from the biofilm reactor after 4 hrs, and a pretreatment process was conducted by treating the samples with 2.5% glutaraldehyde and storing overnight at 4 °C. The samples were dehydrated with solutions of gradually increasing ethanol concentration (70%, 80%, 95%, and 99.9%) and were finally characterized using field-emission SEM (Nova NanoSEM, FEI, USA).

Leaching test

To confirm the covalent binding of CHX, CHX-benzoyl-PPX-modified substrates including Ti6Al4V, SS, PEEK, PMMA, and PS, as well as unmodified such substrates, were soaked in 2 ml PBS (Sigma Aldrich, USA) and were incubated at 37 °C for 30 days. Finally, PBS solutions retrieved from each sample were analysed by using a HPLC-MS/MS system (Agilent Technologies, USA) to identify the trace of CHX concentration.

Cell viability

Commercially available fibroblasts (3T3 clone A31, CCL-163), osteoblasts (7F2, CRL-12557) and preosteoblasts (MC3T3-E1 subclone 4, CRL-2593) were purchased from ATCC, USA and cultured on CHX-benzoyl-PPX-modified and unmodified 48-well cell culture plates (Corning, USA). Cells were seeded at a density of 10^4 cells/cm^2 and were cultured in media containing 10% fetal bovine serum (FBS) for 24 hrs at 37 °C in a humidified atmosphere of 5% CO_2 and 95% air. Experiments were performed in six replicates. For the cell viability assay, 3-[4,5-dimethylthiazol-2-yl]-2,5-diphenyl tetrazolium bromide (MTT) solution (Sigma-Aldrich, USA) was added to each well and incubated for 3 hrs at 37 °C. Subsequently, the MTT solution was aspirated, and the formazan crystals that formed were dissolved in DMSO. The spectrophotometric absorbance at 570 nm was measured using a multi-well plate reader (PowerWave X, BioTek Instruments, USA).

Results and discussion

### Surface modifications and characterizations

A benzoyl-PPX coating was synthesized from 4-benzoyl[2.2]paracyclophane via a refined chemical vapor deposition (CVD) polymerization process under previously reported conditions [28]. During the CVD process, a sublimation temperature of 120-130 °C was used to sublime 4-benzoyl[2.2]paracyclophane, and the sublimated paracyclophanes were transferred to the pyrolysis zone, which exposed the compounds to temperatures of approximately 800 °C and cleaved the *C-C* bonds of the paracyclophanes to generate the corresponding *p*-quinodimethanes (monomers) [37, 38]. During the last step, the monomers polymerized upon condensation on a cooled substrate, forming the benzoyl-PPX coating on the substrate. Substrate materials that are commonly used for biomedical applications, including titanium alloy (Ti6Al4V), stainless steel (SS), polyether ether ketone (PEEK), polymethyl methacrylate (PMMA), and polystyrene (PS), were selected for the CVD coating of benzoyl-PPX in this study. For surface characterization via IRRAS and XPS, benzoyl-PPX was prepared on gold and silicon substrates. A film deposition monitor based on a quartz crystal microbalancing technique was installed in the deposition chamber and was used to confirm the coating thickness during the coating process. A controlled growth rate of approximately 0.5-1 Å·s^{-1} was maintained to ensure the coating quality. Consequently, the thickness of the coating on the substrates was approximately 1000 Å. Uniform and consistent benzoyl-PPX coatings were deposited on the substrates as characterized by ellipsmetry after retrieving the samples from the deposition chamber. With a straightforward coating process, the modification protocol is a facile approach because (i) the immobilization process does not require functional groups on the antibacterial molecules, (ii) the coating decouples the underlying substrate material surface properties and decreases the number of procedures required for

surface modification, and (iii) the CVD polymerization process can produce a conformal coating with a high aspect ratio, which is advantageous for complicated and dedicated bio-devices.
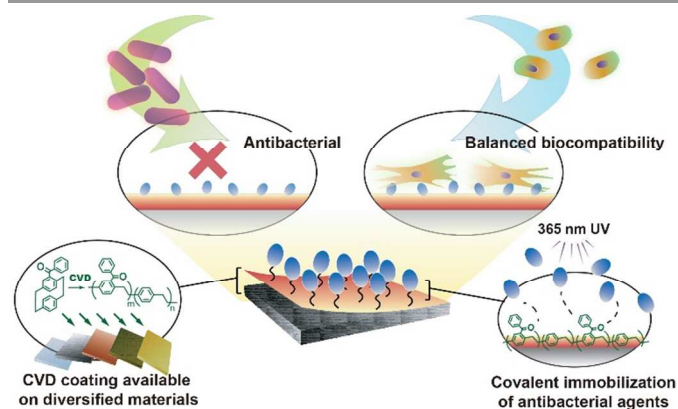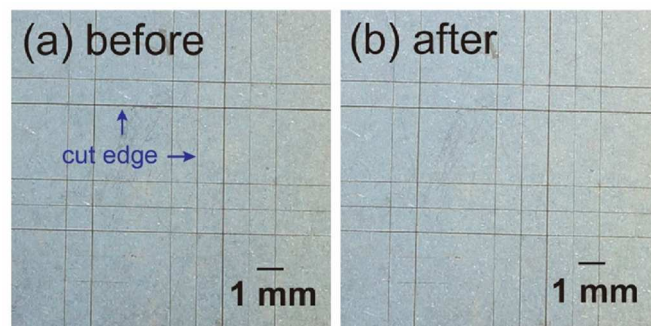

Figure 1. Schematic illustration of CVD polymerization to prepare a photodefinable benzoyl-functionalized poly-p-xylylene coating on various substrates. Antibacterial agents, e.g., CHX molecules, can be covalently immobilized on such coated surfaces. The modified surfaces exhibit effective antibacterial activities and balanced biocompatibility.

Regarding immobilization, benzoyl-PPX contains a photoactive carbonyl group that is analogous to the benzophenone moiety and rapidly crosslinks with CHX molecules via benzophenone triplet insertion into C-H or N-H bonds under approximately 365-nm UV irradiation [28, 39, 40]. The schematic photoimmobilization process is illustrated in **Figure 1**. The resulting CHX-immobilized surface was characterized using IRRAS, and the spectra were compared to bare benzoyl-PPX, as indicated in **Figure 2.** Characteristic peaks at 1604 cm^{-1} and 1667 cm^{-1} were detected for the carbonyl stretches from the benzoyl-PPX (**Figure 2a**). After the photoimmobilization process conjugated the CHX, a weakened 1667 cm^{-1} band was detected in the spectra (**Figure 2a**), and a strong absorption from the C-C-OH group was identified at 1711 cm^{-1}, indicating the excited triplet state [41-43] of benzoyl groups. In addition, peaks at 1568 cm^{-1} and 1510 cm^{-1}, indicative of a C=N group [44]; peaks at 1035 cm^{-1} and 931 cm^{-1}, indicative of a chlorophenyl group; and a band from 3161 cm^{-1} to 3453 cm^{-1}, indicative of a -N-H group, were found for the immobilized CHX molecules.
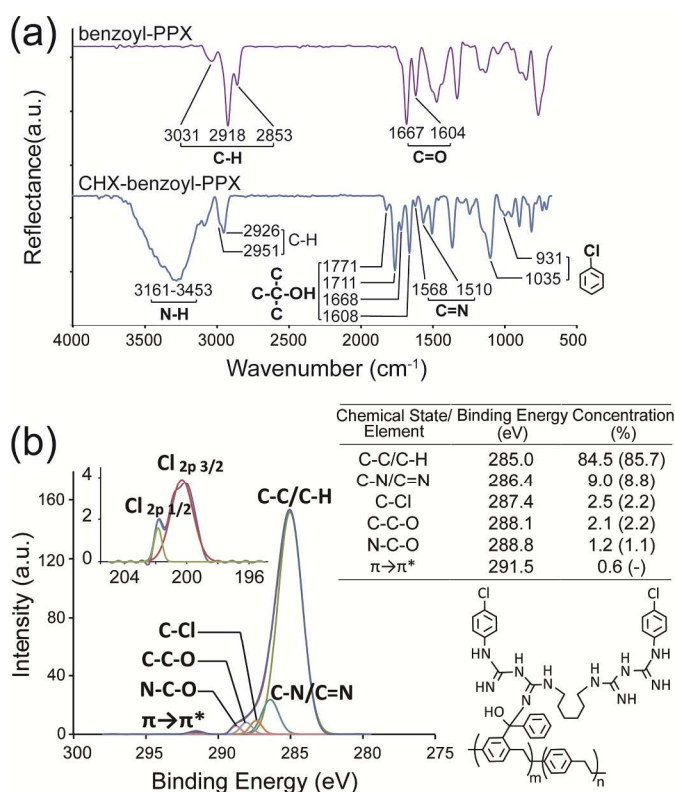
Figure 2. (a) IRRAS spectra of benzoyl-PPX and CHX-benzoyl-PPX. (b) XPS high-resolution C1s and Cl2p analysis of CHX-benzoyl-PPX. The table compares the experimental data with theoretical values (in parentheses).

Figure 3. Images of the cross-cut tape adhesion test on titanium alloy surfaces modified with CHX-benzoyl coating. The images were captured (a) before and (b) after the tape test.

The relative amount of immobilized CHX was estimated using a quartz crystal microbalance system, which monitors adsorbed or conjugated molecules on a crystal sensor surface [45]. Crystal frequencies were measured on the bare crystal surface, at each modification step of benzoyl-PPX coating, and on the CHX-immobilized crystal. Frequency changes were then calculated and converted according to the Sauerbrey equation [46] to estimate the surface density of the benzoyl group (5.30 ± 0.11 nmol·cm^{-2}) and the immobilized CHX (1.40 ± 0.08 nmol·cm^{-2}). An approximate molecular ratio of 3:1 (benzoyl to CHX) was detected. X-ray photoelectron spectroscopy (XPS) was further used to characterize the surface chemical structures of the CHX-immobilized benzoyl-PPX surfaces (hereafter referred to as CHX-benzoyl-PPX). The XPS high-resolution C$_{1s}$ data (**Figure 2b**) show that the experimental values of CHX-benzoyl-PPX were 84.5 atom% for the C-C/H bond, 9.0 atom% for the C-N/C=N bond, 2.5 atom% for the C-Cl bond, 2.1 atom% for the C-C-O bond, and 1.2 atom% for the N-C-O bond. Consequently, the values based on an 3:1 molar ratio of benzoyl moiety to CHX were calculated as 85.7 atom% for the C-C/H bond, 8.8 atom% for the C-N/C=N bond, 2.2 atom% for the C-Cl bond, 2.2 atom% for the C-C-O bond, and 1.1 atom% for the N-C-O bond. These results further confirmed a 3:1 conjugation ratio of the benzoyl functional group with the CHX molecule, showing consistency with QCM results found previously.

The mechanical stability of the CHX-benzoyl-PPX modification coatings on different substrate materials was tested via a cross-cut tape adhesion test. A multi-blade cross-cut tester was used to create two sets of crosswise scratches on the modified substrate, and a piece of Scotch tape was applied and then removed steadily from the scratched samples. A digital camera was used to obtain images of the tested surfaces before and after the tape was removed. **Figure 3** illustrates this comparison for samples with CHX-benzoyl-PPX modification of Ti6Al4V. No discernible damage or delamination was found at the cut edges or on the remaining coating. The results were also evaluated according to the cross-cut scale of ASTM D3359, which classifies film adhesion strength on a scale of 0B to 5B, with 0B corresponding to the weakest adhesion. **Table 1** summarizes the results of the cross-cut tape adhesion test for the CHX-benzoyl-PPX modification of Ti6Al4V, SS, PEEK, PMMA, and PS substrates. The strongest adhesion level, 5B, was found for all substrates tested [47].

Table 1. Cross-cut tape adhesion test of CHX-benzoyl-PPX coating on substrates

Substrate materials	ASTM D3359 Classification
Ti6Al4V	5B
SS	5B
PEEK	5B
PMMA	5B
PS	5B

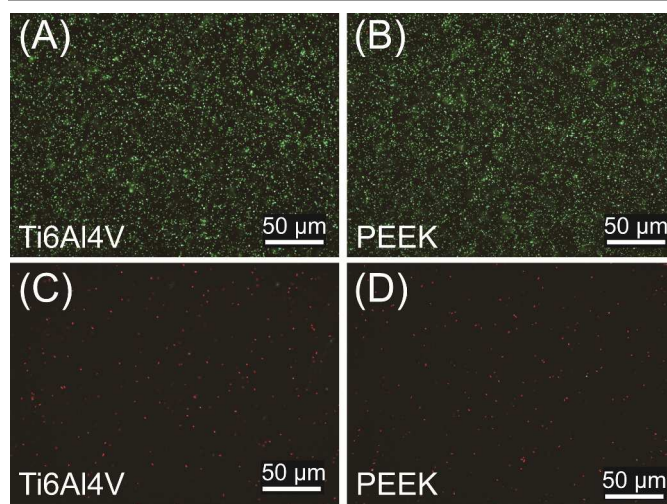### Assessment of antibacterial activities

To examine bacterial adhesion and growth, CHX-benzoyl-PPX-modified Ti6Al4V, SS, PEEK, PMMA, and PS substrates were challenged with an inoculum of *E. cloacae* (10^7 CFU/mL), and an unmodified Ti6Al4V substrate was tested for comparison. The resulting viability of *E. cloacae* was assessed within a 24-hr time frame.
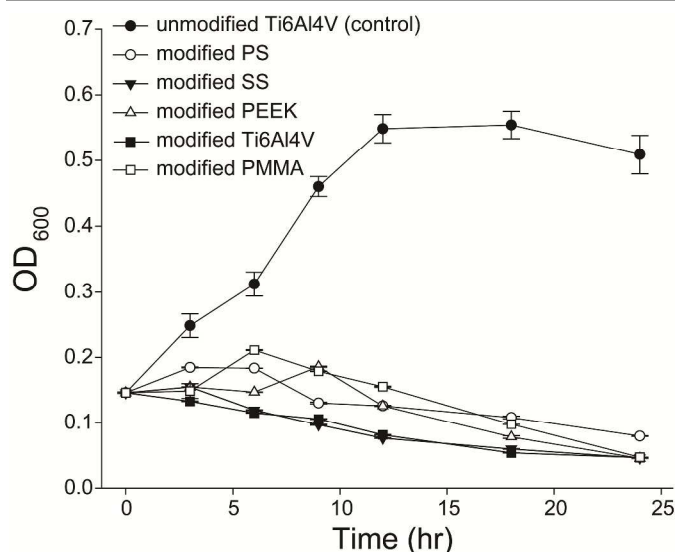
Figure 4. Antibacterial activities of CHX-benzoyl-PPX-modified Ti6Al4V, SS, PEEK, PMMA, and PS substrates and unmodified Ti6Al4V (used as a control surface). The growth curve of *E. cloacae* on these surfaces was recorded over a 24-hr period.
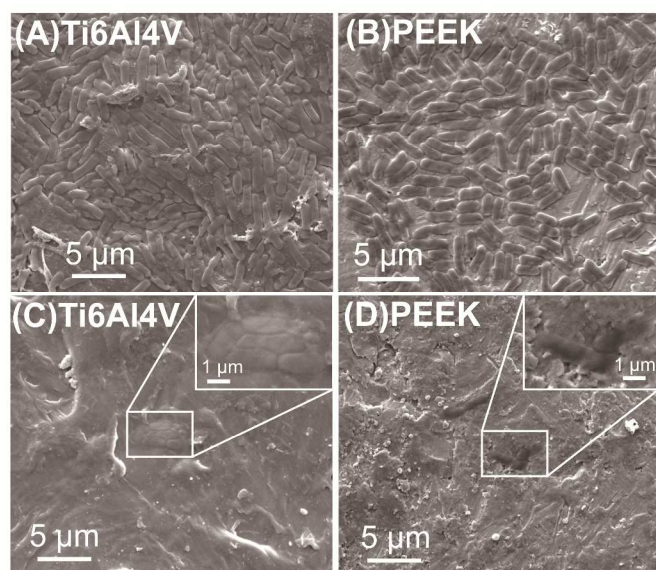

Figure 5. Fluorescence micrographs of LIVE/DEAD viability analysis on (A) unmodified Ti6Al4V, (B) unmodified PEEK, (C) CHX-benzoyl-PPX-modified Ti6Al4V, and (D) CHX-benzoyl-PPX-modified PEEK. The substrates were incubated in an inoculum of *E. cloacae* at 35 °C for 24 hrs. Green signals indicate viable bacteria, and red signals indicate dead or damaged cells.

As shown in **Figure 4**, *E. cloacae* on CHX-benzoyl-PPX-modified substrates exhibited significantly less growth compared to the pronounced growth seen on the unmodified Ti6Al4V substrate. In addition, 6 hr after inoculation, declining growth was observed in the presence of the modified substrates, whereas the unmodified Ti6Al4V substrate exhibited an increase in *E. cloacae* growth, unambiguously confirming that the antibacterial activity of the modified surfaces inhibited rather than delayed the growth of *E. cloacae*. The surface roughness was also studied using a scanning probe microscope (SPM), and the root mean square (RMS) roughness was recorded for Ti6Al4V (9.26 nm), SS (9.14 nm), PEEK (31.65 nm), PMMA (10.93 nm), and PS (3.16 nm). More *E. cloacae* were found on rougher surfaces, such as PEEK and PMMA, consistent with previous studies [48-50]. After the 24-hr *E. cloacae* inoculation test, bacterial viability was further examined using a BacLight LIVE/DEAD kit containing a SYTO 9 dye to stain living bacteria green and a propidium iodide dye to stain dead bacteria red. The CHX-benzoyl-PPX-modified PEEK and Ti6Al4V substrates were chosen for staining and compared with the unmodified substrates. As shown in **Figure 5**, live *E. cloacae* adhered to the surface of unmodified PEEK and Ti6Al4V. In contrast, pronounced red staining was observed on PEEK and Ti6Al4V surfaces that were modified with CHX-benzoyl-PPX, indicating damaged or dead *E. cloacae* on these surfaces. These results further confirm the antibacterial activity of CHX-benzoyl-PPX-modified surfaces.

The colonization of adherent bacteria eventually leads to irreversible biofilm formation, and embedded bacteria are protected from host defences and antibiotic treatments [19, 51, 52]. In this study, the antibacterial activity of CHX-benzoyl-PPX coatings on various substrates was also examined against *E. cloacae* biofilms. A *E. cloacae* biofilm was developed following previously reported procedures [31, 32], that was conducted by seeding bacteria and subsequently feeding replenishing nutrients under a shear flow condition, and forming a biofilm in 2 days. The procedures were performed on modified and unmodified PS, PEEK, PMMA, SS and Ti6Al4V substrates within a bioreactor [30]; verification of the resulting biofilm was performed biochemically by using a crystal violet assay [33, 34] shown in the Electronic Supplementary Information (ESI). The resulting colony formation unit per unit area of the resulting biofilm was calculated and plotted using logarithmic units for each surface, as shown in **Figure 6**.
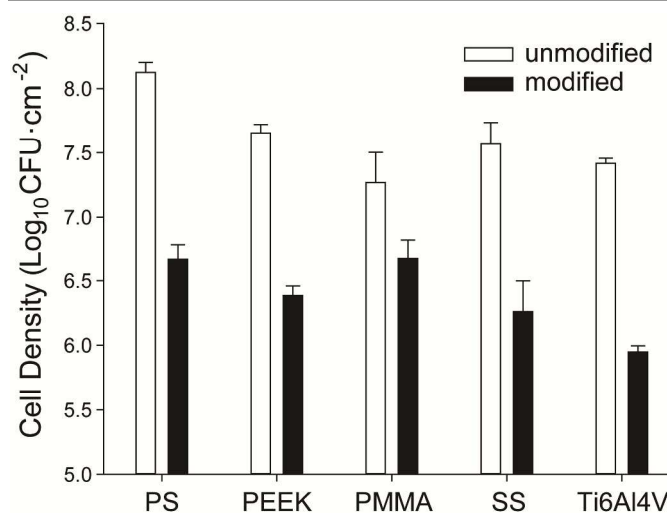
Figure 6. *E. cloacae* biofilm study on CHX-benzoyl-PPX-modified surfaces. The cell density of *E. cloacae* was drastically reduced on CHX-benzoyl-PPX-modified PS (6.68±0.11 $\log_{10} \cdot$CFU cm^{-2}), PEEK (6.39±0.07 $\log_{10} \cdot$CFU·cm^{-2}), PMMA (6.68±0.14 $\log_{10} \cdot$CFU·cm^{-2}), SS (6.26±0.24 $\log_{10} \cdot$CFU·cm^{-2}) and Ti6Al4V (5.95±0.05 $\log_{10} \cdot$CFU·cm^{-2}) compared to a density of 7 − 8 $\log_{10} \cdot$CFU·cm^{-2} on unmodified substrates. Up to a 30-fold reduction in bacterial attachment was estimated for the modified surfaces.

As expected, approximately 7 - 8 $\log_{10} \cdot$CFU·cm^{-2} of *E. cloacae* were discovered on the unmodified surfaces. In contrast, CHX-benzoyl-PPX-modified surfaces, although haven't completely prevented bacterial attachment under biofilm forming conditions, provided reduction to *E. cloacae* biofilm and showed a drastically reduced number of colonization on PS (96.4% reduction), PEEK (94.7 % reduction), PMMA (74.1% reduction), SS (95.1% reduction) and Ti6Al4V (96.6% reduction) surfaces. Moreover, a field emission-scanning electron microscope (FE-SEM) was used to characterize the resulting biofilm-incubated surfaces. CHX-benzoyl-PPX-modified PEEK and Ti6Al4V substrates were chosen for surface characterization and compared with the unmodified surfaces. As shown in the SEM images (**Figure 7**), densely packed and saturated growth patterns of *E. cloacae* were discovered across the surfaces of unmodified PEEK and Ti6Al4V, which is consistent with the greater than 7 $\log_{10} \cdot$CFU·cm^{-2} of bacteria found on the unmodified surfaces in **Figure 6**. However, reduced biofilm formation was evident for CHX-benzoyl-PPX-modified PEEK and Ti6Al4V; aggregates of bacteria were almost absent, and only ruptured cell clusters were observed on these surfaces. These results suggest that the CHX-benzoyl-PPX modification approach can provide the following: (i) effective reduction in bacterial adhesion and the formation of biofilms; and (ii) a wide range of applications on various types of substrates.


Figure 7. SEM micrographs of (A) unmodified Ti6Al4V, (B) unmodified PEEK, (C) CHX-benzoyl-PPX-modified Ti6Al4V, and (D) CHX-benzoyl-PPX-modified PEEK surfaces 4 h after the formation of *E. cloacae* biofilms. Reduction to *E. cloacae* biofilm formation was observed for CHX-benzoyl-PPX-modified surfaces;

ruptured bacterial clusters can be observed. Enlarged views are shown in the top-right corners of (C) and (D).

Cell viability

The important question concerning compatibility of CHX-benzoyl-PPX-modified surfaces with respect to normal cell attachment and proliferation was also examined. The covalently attached CHX not only exhibited remarkable antibacterial properties but also alleviated any concern that CHX will leach residues to the local environment, thus minimizing the impact on surrounding cells and tissues. Antibacterial activities of CHX-benzoyl-PPX-modified surfaces were first verified under preconditioned cell culture medium containing FBS, and the results (data are included in ESI) have confirmed that the surfaces with immobilized CHX are still active in FBS. The responses of cells to the surfaces modified with CHX-benzoyl-PPX were examined. A leaching test was conducted by soaking the modified Ti6Al4V substrates in a buffer solution at 37 °C for 30 days, and no trace of detectable CHX was found, confirming the stable binding of CHX molecules and supporting our previous results of firmly adhered coatings. Cell viability with respect to adhesion to modified surfaces and proliferation was also examined by culturing fibroblasts (3T3), osteoblasts (7F2), and preosteoblasts (MC3T3-E1) on 48-well CHX-benzoyl-PPX-coated cell culture plates for 24 hrs, and the MTT reduction assay was used to characterize the resulting surfaces. The results were compared to unmodified cell culture plates. As shown in **Figure 8**, the MTT assay values for the modified surfaces were normalized to unmodified surface values to determine the cell viabilities for 3T3 (96.6±7.2%), 7F2 (93.2±1.6%), and MC3T3-E1 (98.3±2.7%) cells. Thus, the impact of these modified surfaces on cell viability was limited for all three types of cells tested. Cell proliferation patterns (**Figure 8, (b)-(g)**) were accordingly observed, with analogous cytoskeleton morphology adhering on modified surfaces compared to the unmodified surfaces. Taken together, these results diminish any concern that antibacterial agents, such as CHX molecules, will be leached. Thus, a covalently bound low concentration (1.40±0.08 nmol/cm^2 by QCM analysis) of CHX can provide balanced biocompatibility with the surrounding cells and tissues.
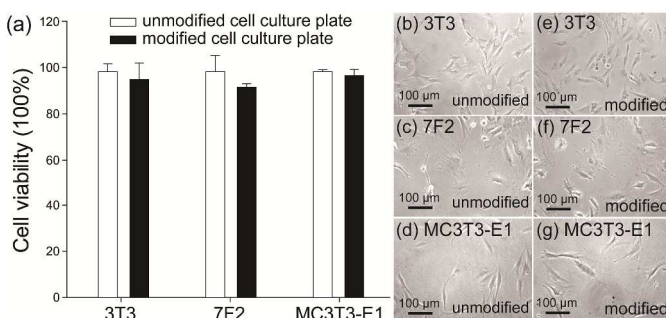
Figure 8. Normal cell viability analysis on CHX-benzoyl-PPX-modified surfaces. Fibroblasts (3T3), osteoblasts (7F2), and preosteoblasts (MC3T3-E1) were cultured on modified surfaces, and the results of the MTT reduction assay are shown in (a). Cell viabilities of 96.6±7.2% for 3T3, 93.2±1.6% for 7F2, and

98.3±2.7% for MC3T3-E1 cells were observed on the modified surfaces. Microscopic images in (b)-(g) are showing cytoskeleton morphology of adhered cells on CHX-benzoyl-PPX-modified and unmodified surfaces. Analysis and observation were performed after 24 hrs of cell culture.

Conclusions

With advancing biomaterial designs and more complicated devices being manufactured for biomedical use, new approaches to preventing infection that are tailored to specific materials or devices have shown promising results, wide applicability, and a reduced risk of toxicity from antibacterial substances. The treatment technology reported here was designed with these aims. We have demonstrated the covalent attachment of the antibacterial compound chlorhexidine and studied the resulting antibacterial activities on various substrate materials. With an established library of antibiotics and the availability of new antibacterial agents, this coating technology may be broadly applicable for attaching other agents to a diverse range of materials and devices according to the specific application. In the future, we plan to perform clinical studies to further evaluate this technology.

Acknowledgements

Notes and references

[a] Department of Orthopedic Surgery, National Taiwan University Hospital and National Taiwan University College of Medicine, Taipei 10018, Taiwan.

[b] Department of Chemical Engineering, National Taiwan University, Taipei 10617, Taiwan.

[c] Department of Biochemical Science and Technology, National Taiwan University, Taipei 10617, Taiwan.

± Shu-Yun Yeh and Bing-Heng Lee contributed equally.

*To whom correspondence should be addressed: hsychen@ntu.edu.tw

† Electronic Supplementary Information (ESI) available: biochemical crystal violet assay and preconditioned antibacterial test data. See DOI: 10.1039/b000000x/

1. D. Campoccia, L. Montanaro and C. R. Arciola, *Biomaterials*, 2006, **27**, 2331-2339.
2. R. O. Darouiche, *New England Journal of Medicine*, 2004, **350**, 1422-1429.
3. C. R. Arciola, D. Campoccia, P. Speziale, L. Montanaro and J. W. Costerton, *Biomaterials*, 2012, **33**, 5967-5982.
4. T. Abee, Á. T. Kovács, O. P. Kuipers and S. van der Veen, *Current Opinion in Biotechnology*, 2011, **22**, 172-179.
5. P. A. Norowski and J. D. Bumgardner, *Journal of Biomedical Materials Research Part B: Applied Biomaterials*, 2009, **88B**, 530-543.
6. L. Rodrigues, in *Bacterial Adhesion*, eds. D. Linke and A. Goldman, Springer Netherlands, 2011, pp. 351-367.
7. T. He, Z. L. Shi, N. Fang, K. G. Neoh, E. T. Kang and V. Chan, *Biomaterials*, 2009, **30**, 317-326.
8. R. Müller, A. Eidt, K.-A. Hiller, V. Katzur, M. Subat, H. Schweikl, S. Imazato, S. Ruhl and G. Schmalz, *Biomaterials*, 2009, **30**, 4921-4929.
9. Z. Shi, K. G. Neoh, E. T. Kang, C. Poh and W. Wang, *Journal of Biomedical Materials Research Part A*, 2008, **86A**, 865-872.
10. X. Ding, C. Yang, T. P. Lim, L. Y. Hsu, A. C. Engler, J. L. Hedrick and Y.-Y. Yang, *Biomaterials*, 2012, **33**, 6593-6603.
11. Z. C. Ruhe, D. A. Low and C. S. Hayes, *Trends in Microbiology*, 2013, **21**, 230-237.
12. A. Agarwal, T. B. Nelson, P. R. Kierski, M. J. Schurr, C. J. Murphy, C. J. Czuprynski, J. F. McAnulty and N. L. Abbott, *Biomaterials*, 2012, **33**, 6783-6792.
13. Z. Chen, B. J. Chisholm, S. Stafslien, J. He and S. Patel, *Journal of Biomedical Materials Research Part A*, 2010, **95A**, 486-494.
14. J. A. Lemire, J. J. Harrison and R. J. Turner, *Nature Reviews Microbiology*, 2013, **11**, 371-384.
15. D. Campoccia, L. Montanaro and C. R. Arciola, *Biomaterials*, 2013, **34**, 8533-8554.
16. G. Bedoux, B. Roig, O. Thomas, V. Dupont and B. Bot, *Environ Sci Pollut Res*, 2012, **19**, 1044-1065.
17. G. F. Calogiuri, E. Di Leo, A. Trautmann, E. Nettis, A. Ferrannini and A. Vacca, *Journal of Allergy & Therapy*, 2013, **4**, 1-7.
18. D. C. Coraça-Huber, M. Fille, J. Hausdorfer, K. Pfaller and M. Nogler, *Journal of Applied Microbiology*, 2012, **112**, 1235-1243.
19. V. Antoci Jr, C. S. Adams, J. Parvizi, H. M. Davidson, R. J. Composto, T. A. Freeman, E. Wickstrom, P. Ducheyne, D. Jungkind, I. M. Shapiro and N. J. Hickok, *Biomaterials*, 2008, **29**, 4684-4690.
20. H. Murata, R. R. Koepsel, K. Matyjaszewski and A. J. Russell, *Biomaterials*, 2007, **28**, 4870-4879.
21. G. McDonnell and A. D. Russell, *Clin Microbiol Rev*, 1999, **12**, 147-179.
22. M. Puig-Silla, J. M. Montiel-Company and J. M. Almerich-Silla, *Medicina Oral Patologia Oral Y Cirugia Bucal*, 2008, **13**, E257-E260.
23. S. Jenkins, M. Addy and W. Wade, *Journal of Clinical Periodontology*, 1988, **15**, 415-424.
24. H.-Y. Chen, J.-M. Rouillard, E. Gulari and J. Lahann, *Proceedings of the National Academy of Sciences*, 2007, **104**, 11173-11178.
25. M.-G. Wu, H.-L. Hsu, K.-W. Hsiao, C.-C. Hsieh and H.-Y. Chen, *Langmuir*, 2012, **28**, 14313-14322.
26. H.-Y. Chen and J. Lahann, *Analytical Chemistry*, 2005, **77**, 6909-6914.
27. W. W. Shen, S. G. Boxer, W. Knoll and C. W. Frank, *Biomacromolecules*, 2001, **2**, 70-79.
28. K. Y. Suh, R. Langer and J. Lahann, *Advanced Materials*, 2004, **16**, 1401-1405.
29. A. D3359-02, *ASTM International*.
30. C. F. Lee, C. J. Lee, C. T. Chen and C. T. Huang, *J Photochem Photobiol B*, 2004, **75**, 21-25.
31. G. Ramage, B. L. Wickes and J. L. Lopez-Ribot, *Revista iberoamericana de micologia*, 2008, **25**, 37-40.
32. C.-F. Lee, C.-J. Lee, C.-T. Chen and C.-T. Huang, *Journal of Photochemistry and Photobiology B: Biology*, 2004, **75**, 21-25.
33. S. Stepanović, D. Vuković, I. Dakić, B. Savić and M. Švabić-Vlahović, *Journal of Microbiological Methods*, 2000, **40**, 175-179.
34. X. Li, J. Yan Z Fau - Xu and J. Xu.
35. H. J. Harmsen, G. R. Gibson, P. Elfferich, G. C. Raangs, A. C. Wildeboer-Veloo, A. Argaiz, M. B. Roberfroid and G. W. Welling, *FEMS microbiology letters*, 2000, **183**, 125-129.
36. Y. Moreno, M. C. Collado, M. A. Ferrús, J. M. Cobo, E. Hernández and M. Hernández, *International Journal of Food Science & Technology*, 2006, **41**, 275-280.
37. W. F. Gorham, *Journal of Polymer Science Part A-1: Polymer Chemistry*, 1966, **4**, 3027-3039.
38. J. Lahann and R. Langer, *Macromolecules*, 2002, **35**, 4380-4386.
39. A. A. Lin, V. R. Sastri, G. Tesoro, A. Reiser and R. Eachus, *Macromolecules*, 1988, **21**, 1165-1169.
40. M. V. Encinas and J. C. Scaiano, *Journal of the American Chemical Society*, 1981, **103**, 6393-6397.

41. F. S. Li, S. X. Zhou, B. You and L. M. Wu, *Journal of Applied Polymer Science*, 2006, **99**, 3281-3287.
42. F. S. Li, S. X. Zhou, B. You and L. M. Wu, *Journal of Applied Polymer Science*, 2006, **99**, 1429-1436.
43. C.-T. Su, R.-H. Yuan, Y.-C. Chen, T.-J. Lin, H.-W. Chien, C.-C. Hsieh, W.-B. Tsai, C.-H. Chang and H.-Y. Chen, *Colloids and Surfaces B: Biointerfaces*, 2014, **116**, 727-733.
44. L. Chen, L. Bromberg, T. A. Hatton and G. C. Rutledge, *Polymer*, 2008, **49**, 1266-1275.
45. K. A. Marx, *Biomacromolecules*, 2003, **4**, 1099-1120.
46. G. Sauerbrey, *Z. Physik*, 1959, **155**, 206-222.
47. H.-Y. Sun, C.-Y. Fang, T.-J. Lin, Y.-C. Chen, C.-Y. Lin, H.-Y. Ho, M. H. C. Chen, J. Yu, D.-J. Lee, C.-H. Chang and H.-Y. Chen, *Advanced Materials Interfaces*, 2014, n/a-n/a.
48. N. J. Hallab, K. J. Bundy, K. O'Connor, R. L. Moses and J. J. Jacobs, *Tissue Eng*, 2001, **7**, 55-71.
49. M. Gharechahi, *Journal of Biomaterials and Nanobiotechnology*, 2012, **03**, 541-546.
50. K. Kawai, M. Urano and S. Ebisu, *Journal of Prosthetic Dentistry*, 2000, **83**, 664-667.
51. J. Amalric, P. H. Mutin, G. Guerrero, A. Ponche, A. Sotto and J.-P. Lavigne, *Journal of Materials Chemistry*, 2009, **19**, 141-149.
52. S. Leprêtre, F. Chai, J.-C. Hornez, G. Vermet, C. Neut, M. Descamps, H. F. Hildebrand and B. Martel, *Biomaterials*, 2009, **30**, 6086-6093.

TABLE OF CONTENTS ENTRY

Covalent immobilization of antibacterial agents
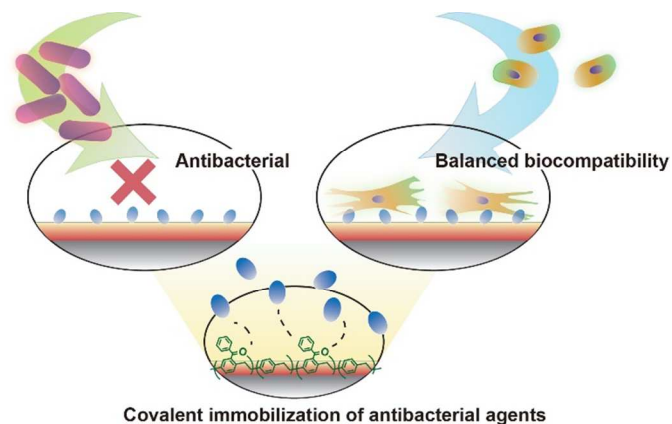
An advanced antibacterial modification technique is conducted by immobilizing antibacterial agents using vapor-deposited parylene coatings to result in effective reduction in bacteria attachment and show balanced biocompatibility.